Disparate roles of ATR and ATM in immunoglobulin class switch recombination and somatic hypermutation

Qiang Pan-Hammarström,[1] Aleksi Lähdesmäki,[1] Yaofeng Zhao,[1] Likun Du,[1] Zhihui Zhao,[1] Sicheng Wen,[1] Victor L. Ruiz-Perez,[2] Deborah K. Dunn-Walters,[3] Judith A. Goodship,[2] and Lennart Hammarström[1]

[1]Division of Clinical Immunology, Department of Laboratory Medicine, Karolinska University Hospital, Huddinge, SE-14186 Stockholm, Sweden
[2]Institute of Human Genetics, Newcastle University, Newcastle-upon-Tyne NE1 3B2, England, UK
[3]Dept. of Immunobiology, King's College London School of Medicine, Guy's Hospital, London SE1 9RT, England, UK

Class switch recombination (CSR) and somatic hypermutation (SHM) are mechanistically related processes initiated by activation-induced cytidine deaminase. Here, we have studied the role of ataxia telangiectasia and Rad3-related protein (ATR) in CSR by analyzing the recombinational junctions, resulting from in vivo switching, in cells from patients with mutations in the *ATR* gene. The proportion of cells that have switched to immunoglobulin (Ig)A and IgG in the peripheral blood seems to be normal in ATR-deficient (ATRD) patients and the recombined S regions show a normal "blunt end-joining," but impaired end joining with partially complementary (1–3 bp) DNA ends. There was also an increased usage of microhomology at the μ-α switch junctions, but only up to 9 bp, suggesting that the end-joining pathway requiring longer microhomologies (≥10 bp) may be ATR dependent. The SHM pattern in the Ig variable heavy chain genes is altered, with fewer mutations occurring at A and more mutations at T residues and thus a loss of strand bias in targeting A/T pairs within certain hotspots. These data suggest that the role of ATR is partially overlapping with that of ataxia telangiectasia–mutated protein, but that the former is also endowed with unique functional properties in the repair processes during CSR and SHM.

CORRESPONDENCE
Qiang Pan-Hammarström:
Qiang.Pan-Hammarstrom@ki.se

Abbreviations used: AID, activation-induced cytidine deaminase; A-T, ataxia-telangiectasia; ATM, ataxia telangiectasia mutated; ATR, ataxia telangiectasia and Rad3-related protein; ATRD, ATR-deficient; ATRIP, ATR-interacting protein; C, constant; CSR, class switch recombination; DSB, double-strand break; HR, homologous recombination; NHEJ, nonhomologous end joining; PIKK, phosphoinositol 3-kinase–like kinase; S, switch; SHM, somatic hypermutation; ssDNA, single-stranded DNA; V, variable; VH, Ig variable heavy chain.

Maintenance of genome stability depends on an appropriate response to DNA damage and, when insufficient, may lead to development of neoplasia. A double-strand break (DSB) is thought to be one of the most severe forms of DNA damage. There are two major types of DSB repair mechanisms: homologous recombination (HR) and nonhomologous end joining (NHEJ). The fundamental difference between HR and NHEJ is the dependence on DNA homology in the former. HR is considered error free and is most active in the late S/G2 phase of the cell cycle. NHEJ, on the other hand, utilizes little or no sequence homology and is active throughout the whole cell cycle. Proteins known to be involved in NHEJ include Ku70, Ku80, DNA-PKcs, artemis, the Mre11–Rad50–Nbs1 complex, DNA ligase IV, and XRCC4 (1).

During development of the immune system, mechanisms for genomic stability are exploited to generate genetic diversity. During early T and B lymphocyte development, V(D)J recombination takes place to assemble variable (V) exons of the T cell receptor and Ig genes, respectively, giving rise to a large repertoire of specificities. In B cells, two additional mechanisms, which are activated after antigen recognition, further diversify the antibody response: class switch recombination (CSR) and somatic hypermutation (SHM). CSR allows a previously rearranged Ig heavy chain V domain to be expressed in association with a different constant (C) region, leading to production of different isotypes (IgG, IgA or IgE), without changing the antibody specificity. In SHM, the V domains of immunoglobulins may increase their affinity by accumulation of mutations.

CSR and SHM are both initiated by a single B cell–specific factor, activation-induced cytidine deaminase (AID) (2), probably by deamination of dC residues within the Ig locus (3–5). Depending on which way the initial dU/dG

The online version of this article contains supplemental material.

mismatch is resolved, it will result in introduction of mutations in the V region genes (SHM) or recombination of the two switch (S) regions (CSR). At least three pathways (NHEJ, base excision repair, and mismatch repair) have been implicated in processing, repair, and ligation of the broken DNA ends (for review see reference 6). However, the way in which these pathways are regulated and coordinated to mediate CSR and /or SHM are still not well understood.

The ataxia telangiectasia mutated (ATM) protein, a phosphoinositol 3-kinase–like kinase (PIKK), is a master regulator of the DSB response signal transduction pathway. This kinase has been suggested to have a role in CSR, as patients with ataxia-telangiectasia (A-T), who carry mutations in *ATM* (7), frequently show deficiency of serum IgA, IgG2, IgG4, and IgE (8). The Sμ-Sα recombination junctions from A-T patients are characterized by a strong dependence on microhomologies and are devoid of normally occurring mutations around the breakpoint, suggesting that ATM might be directly involved in the end joining process in CSR (9). Recently, ATM (10, 11) and its three substrates, Nbs1 (9, 12–15), H2AX (16), and 53BP1 (17, 18) have all been implicated in CSR, further supporting the notion that ATM-depended pathways are involved in the recombination process.

The CSR defect in NBS- or 53BP1-deficient cells appears more severe than in ATM-deficient cells (9, 17), suggesting possible roles for other upstream PIKKs in CSR. Indeed, DNA-PKcs (DNA-dependent protein kinase catalytic subunit) has been implicated in both V(D)J recombination and CSR (19, 20), possibly through its role in NHEJ. Another more closely related PIKK, ataxia telangiectasia and Rad3-related protein (ATR), which shares several substrates with ATM (21) (including H2AX and 53BP1), could potentially respond to DNA damage in a redundant or overlapping manner. Its role in CSR, however, has not been possible to study, as loss of ATR in mice results in embryonic lethality (22, 23).

The SHM process is largely normal in cells deficient in ATM (24), H2AX(16), 53BP1(17), and DNAPKcs (25), suggesting that the ATM-dependent pathways and the classical NHEJ pathway are probably dispensable for this process. The role of ATR in SHM has, however, not been possible to study because of lack of a suitable experimental system.

Recently, two consanguineous families with Seckel syndrome were found to carry mutations in the *ATR* gene (26). This syndrome is a rare autosomal recessive disorder characterized by intrauterine growth retardation, dwarfism, microcephaly, "bird-like" facial features, and mental retardation. A subgroup of patients with Seckel syndrome may also manifest pancytopenia (27), chromosomal instability (27, 28), and hematological malignancies (29). To search for a potential functional role of ATR in CSR and SHM, we performed a detailed analysis of μ-α switch (S) recombination junctions and base pair substitutions in Ig variable heavy chain (VH) genes, in cells from three of the five ATR-deficient (ATRD) patients identified to date.

RESULTS

The numbers of clones switched to IgA in ATRD patients are normal

The number of Sμ-Sα fragments was determined from 10 PCR reactions run in parallel, using DNA (30 ng per reaction) from the same individual. This method can be used to estimate the number of clones that have switched to IgA (30). Because of the polyclonal nature of the rearrangements at the Sμ-Sα region, differently sized switch fragments are amplified and visualized. The number of clones that have switched from IgM to IgA in ATRD patients appears to be similar to controls. A typical run is shown in Fig. 1, where at least 11 distinct Sμ-Sα fragments were amplified from the control and at least 10 fragments were amplified from the ATRD1 patient. The experiments were repeated three times for each patient. The average numbers of Sμ-Sα fragments generated from ATRD1 and ATRD2 were 11.3 and 8.7, respectively, with an average of 10.0, which is similar to controls (7–15, average:11.8). Thus, the proportion of cells that have switched to IgA in the peripheral blood in ATRD patients, at the time of sampling, appears to be normal.

Sμ–Sα recombination junctions in ATRD patients

We subsequently cloned and sequenced 40 S fragments (39 Sμ-Sα and 1 Sμ-Sγ-Sα) from ATRD1 and ATRD2, generated in the aforementioned PCR reactions. All the S fragment sequences were unique and therefore represent independent CSR events (Fig. S1, available at http://www.jem.org/cgi/content/full.jem20050595/DC1). The S junctions from controls (n = 154), used for comparison, have been published previously (9, 13).

Switching to α1 occurred more frequently than to α2 in ATRD patients as compared with controls (80 vs. 66%). However, this difference was not statistically significant. The frequency of additional intra-Sα region recombination, as judged by the number of Sμ-Sα-Sα fragments identified, seems to be slightly reduced as compared with controls (5 and 11%, respectively), but not to a significant degree.

We subsequently analyzed the microhomology usage at the Sμ-Sα junctions in the ATRD patients. There was a significant increase in the extent of donor–acceptor homology at the Sμ-Sα junctions from ATRD patients; the average length of overlap being 3.0 ± 3.8 bp in ATRD and 1.8 ± 3.2 bp in control B cells ($P < 0.05$, Student's t test). The junctions from ATRD patients showed a significantly increased usage of microhomology (≥4 bp) (Table I, 26 + 10 + 3 = 39 vs. 20% in controls, χ^2 test, $P < 0.05$) as compared with controls. Interestingly, this was mainly because of homologies encompassing 4–6 bp (separated in Fig. 2 A, 26 vs. 10% in controls, χ^2 test, $P < 0.01$) and, to a much lesser degree, 7–9 bp. However, there was no increased usage of longer microhomologies (i.e., ≥10 bp) at the junctions from the patients as compared with controls (Fig. 2 A and Table I). When the data was plotted as an accumulative curve, it is evident that the proportion of S junctions with longer homologies was almost the same as in controls (Fig. 2 B).

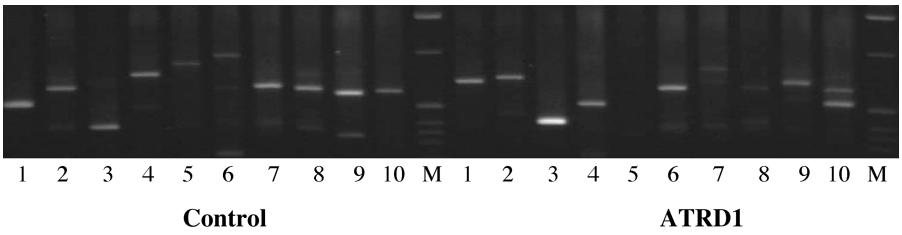

Figure 1. Amplification of Sμ-Sα breakpoints. A typical run for control and ATRD patient. The numbers of μ-α switch fragments were determined from 10 PCR reactions run in parallel (lanes 1–10). 11 fragments can be seen in the control (lane 9 has two distinct bands) and 10 in ATRD1 (lane 5 has none and lane 10 has two distinct bands). M, molecular weight marker.

Mutations at or close to the Sμ-Sα junctions (±15 bp) from ATRD patients

In ATRD patients, the number of S junctions with mutations was significantly smaller than in controls (18 vs. 39%, χ^2 test, $P < 0.05$), whereas insertions were observed at a similar rate (23 vs. 25%) (Table I). The frequencies of mutations or insertions around the junctions were 13.7 and 22.9/1,000 bp for ATRD and controls, respectively. The number of mutations and insertions available for analysis was too low in the patient group ($n = 13$) to allow a formal analysis of the pattern of nucleotide alterations.

Mutations in the Sμ region (>15 bp upstream of the switch junctions) in ATRD patients

The mutation pattern in the Sμ region (upstream of the breakpoints, referred to as SHM-like mutations) resembles that in the V regions and is clearly different from that at, or close to, the Sμ-Sα breakpoints (13, 24), suggesting that the former mutations occur at an early step during CSR (12). In ATRD patients, SHM-like mutations in the Sμ region were observed at a significantly lower frequency than in controls (3.1/1,000 bp vs. 6.5/1,000 bp; χ^2 test, $P < 0.001$). In the few mutations observed ($n = 25$), the general pattern of base substitution seems to be slightly different from controls, with a stronger, but statistically nonsignificant, preference for G/C sites (72 vs. 62% in controls), a reduced number of mutations at A nucleotides (12 vs. 21% in controls) and an increased frequency of mutations at G nucleotides (40 vs. 28%).

The mutations in the Sμ region from ATRD patients were less often associated with the previously described consensus hotspot for SHM, the RGYW/WRCY (R = A or G, Y = C or T, W = A or T) motif (31), as compared with controls (56 and 70% for ATRD and controls, respectively), but not to a significant degree.

Characterizations of Sμ-Sγ junctions in ATRD patients

We have previously designed a series of PCRs that specifically amplify Sμ-Sγ1, Sμ-Sγ2, and Sμ-Sγ3 fragments from DNA from peripheral blood cells. The number of clones that have switched to the different IgG subclasses in ATRD patients appears to be similar to controls (not depicted). We subsequently cloned and sequenced 49 Sμ-Sγ fragments from the ATRD patients. 48 of these fragments were unique in their junctional sequences and most were a result of direct switching to IgG1 ($n = 17$), IgG2 ($n = 8$), or IgG3 ($n = 23$). One S fragment was a result of sequential switching to IgG2 through Sα1.

Table I. Characterization of Sμ-Sα and Sμ-Sγ junctions[a,b]

	Perfectly matched short homology					Mutation at S junctions	1-bp insertion at S junctions	Total no. of S fragments
	0 bp	1–3 bp	4–6 bp	7–9 bp	≥10 bp			
Sμ-Sα								
Controls	67 (44%)	56 (36%)	15 (10%)	11 (7%)	5 (3%)	60 (39%)	39 (25%)	154
ATRD	16 (41%)	8 (21%)	**10 (26%)**[c]	4 (10%)	1 (3%)	**7 (18%)**[d]	9 (23%)	39
A-T	**2 (5%)**[e]	15 (34%)	9 (21%)	5 (11%)	**13 (30%)**[e]	**5 (11%)**[e]	**1 (2%)**[e]	44
Sμ-Sγ								
Controls	19 (32%)	37 (63%)	3 (5%)	0 (0%)	0 (0%)	24 (41%)	6 (10%)	59
ATRD	15 (32%)	25 (53%)	5 (11%)	2 (4%)	0 (0%)	13 (28%)	6 (13%)	47
A-T	6 (16%)	23 (61%)	**7 (18%)**[d]	2 (5%)	0 (0%)	**7 (18%)**[d]	3 (8%)	38

[a]Statistical analysis was performed using χ^2 test. Statistically significant differences are bold.
[b]Parts of the data from A-T patients and controls have been described previously (references 9, 13, 45).
[c]$P < 0.01$.
[d]$P < 0.05$.
[e]$P < 0.001$.

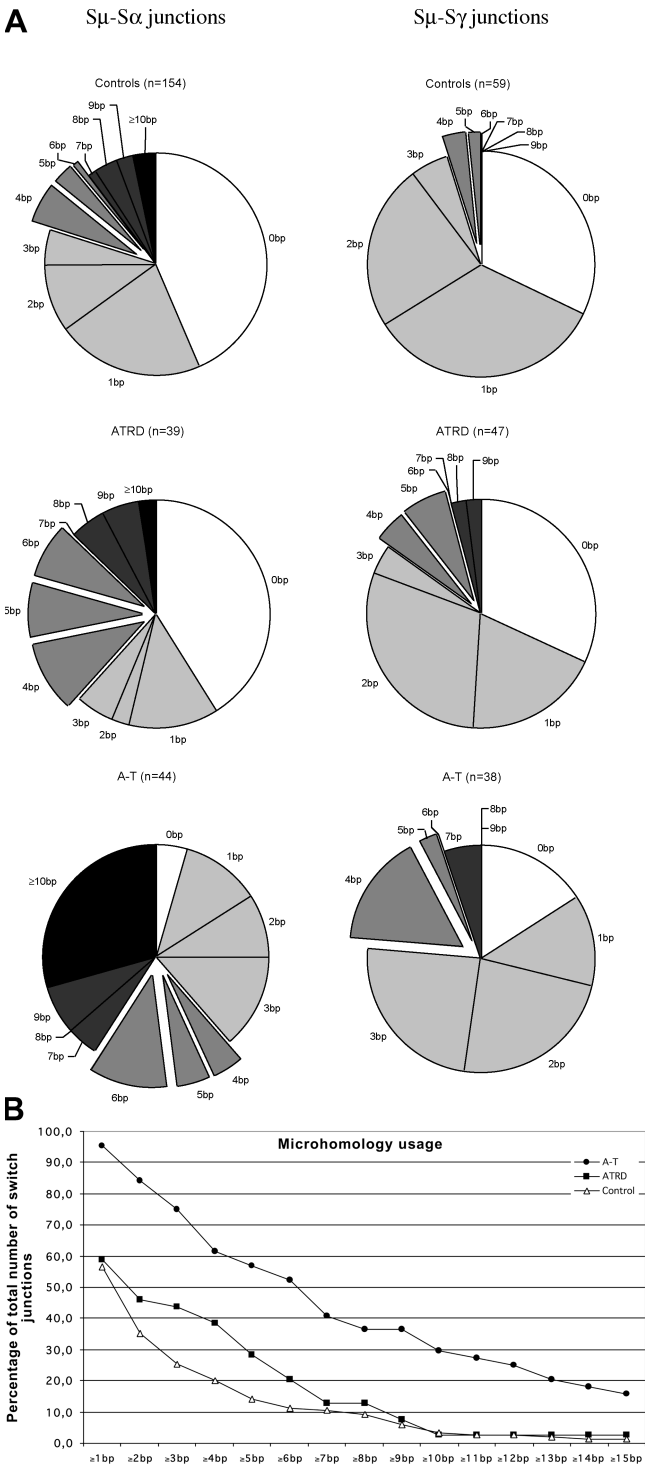

Figure 2. Microhomology usage at Sμ-Sα and Sμ-Sγ junctions. (A) Pie charts demonstrate the perfectly matched short homology usage at Sμ-Sα and Sμ-Sγ junctions in controls, ATRD, and A-T patients. The proportion of switch junctions with a given size of perfectly matched short homology is indicated by the size of the slices. For clarity, the 4–6 bp homology portion, which significantly differs between ATRD and controls, is separated from the pie. (B) Accumulative curves indicate the microhomology usage at Sμ-Sα junctions in controls, ATRD and A-T patients. The percentage of all switch junctions with a given size, using perfectly matched short homology, is plotted.

As in the Sμ-Sα junctions, there was a significant increase in donor–acceptor homology at the Sμ-Sγ junctions from ATRD patients (the average length of overlap being 1.8 ± 2.0 bp vs. 1.2 ± 1.2 bp in controls; $P < 0.05$, Student's *t* test). There was a trend toward an increased usage of microhomologies (≥4 bp) in the ATRD patients, but not to a statistically significant degree (Fig. 2 A and Table I, 11 + 4 + 0 = 15 vs. 5% in controls). Furthermore, the number of Sμ-Sγ junctions that showed mutations (±15 bp) was lower as compared with in controls (28 vs. 41%), whereas insertions were observed at a similar rate (13 vs. 12%).

Analysis of mutations in VH-Cγ transcripts in ATRD patients

RNA was prepared from PBLs of all three patients. In the first set of experiments, a previously described PCR strategy (24) was used to amplify the VH3-Cγ transcripts from ATRD3. In total, 14 distinct VH-Cγ clones were generated and the majority of these clones carried at least 10 mutations. The average frequency of mutations in the VH genes derived from this patient was 9.2%, which is higher than that found previously in normal controls ($n = 7$, 1.5–6.6%, average 4.2%) (24). One notable finding was that the A and T residues on the coding strand were targeted at a similar frequency in the patient (21.9 and 20.8%, respectively; 365 mutations) and thus did not display the DNA strand polarity observed in controls (29.6 and 13.6%, respectively; 619 mutations).

To verify these findings, we performed a second set of experiments, where all three patients were included. VH3-23-Cγ transcripts were selectively amplified to exclude the possibility that the difference in A/T base targeting observed were because of a differential usage of VH3 genes between patients and controls. In total, 33 and 40 distinct VH3-23-Cγ clones were generated from B cells of ATRD patients and controls, respectively (Table II). Most of the VH3-23 clones from the patients were mutated (2–49 bp substitutions/clone) and only 6% of the VH3-23 genes exhibited unmutated sequences (0–1 bp substitutions/clone) (Fig. 3 A). The frequency of mutations in the VH3-23 genes derived from ATRD patients varied from 6.8 to 11.9%, which is similar to, or slightly higher than, the age-matched control donors (Table II). The ratio of replacement vs. silent mutations (R/S) in CDRs and framework regions was similar in the patient and control groups, arguing against any major abnormalities in the antibody selection process in ATRD patients.

The distribution of mutations observed in ATRD patients (754 mutations in total, 22.8/VH) was largely similar to that found in normal controls (749 mutations in total, 18.7/VH), with major hotspots of mutation (AGC and GCT at codons Ser[32], Ala[55], and Ser[62]), conforming to the previously described hotspot consensus RGYW/WRYC motif (31) (Fig. 3 B). The mutations showed a preference for transitions in both patients and controls (53 and 56%, respectively).

Table II. Mutations in VH3-23-Cγ transcripts from PBL from ATRD patients and controls[a]

		Clones			Mutations in V region		Clustering ratio	R/S	
	Age (yr)	All	Distinct	Unmutated	Total	% bp	CDR/FR[b]	CDRs	FRs
ATRD patients									
ATRD1	25	15	13	0	302	8.6	0.73	3.4	1.8
ATRD2	13	15	14	2	258	6.8	0.73	3.7	1.7
ATRD3	15	6	6	0	194	11.9	0.62	3.9	2.0
Total		36	33	2	754	8.4	0.70	3.6	1.8
Controls									
C1	14	12	11	1	100	3.4	1.22	5.9	1.5
C2	adult	11	11	0	275	9.3	0.73	4.5	1.7
C3	28	6	6	0	147	9.0	0.69	5.7	2.0
C4	24	8	8	0	178	8.2	0.51	14.0	2.2
C5	30	4	4	0	49	4.5	0.53	[c]	1.1
Total		41	40	1	749	6.9	0.70	6.2	1.8

[a]Total RNA was prepared from PBL from all the patients and controls, except for donor C2; buffycoat was obtained and CD27 positive B cells were used.
[b]FR, framework region.
[c]Too few mutations to give a reliable ratio.

However, there were significantly more transitions occurring at T residues in ATRD patients as compared with those in controls (11.1 vs. 7.7%, χ^2 test, $P < 0.05$). Furthermore, as observed in the VH3 sequences from the first set of experiments, the A and T residues on the coding strand were targeted at a similar frequency (after correcting for base composition, 25.6 and 23.0%, respectively) and thus, the DNA strand polarity observed in controls was lost (29.9 and 16.8%, respectively) (Fig. 3 C).

To search for a potential difference in the targeting of specific sequences between the patients and controls, we first analyzed the frequency of mutations in the RGYW/WRYC motifs. A significantly higher than expected number of mutations (18%) was observed within these motifs, both in patients and controls (36 and 38%, respectively, χ^2 test, $P < 0.0001$). However, there seems to be no major difference in targeting of the individual bases in these motifs between the patients and controls. We subsequently analyzed the targeting of the WA/TW motifs and the frequency of mutations within these motifs was almost identical between patients and controls (262/754 vs. 261/749, 34%). TA was the most targeted motif in both patients and controls. However, there was a significant difference in the targeting of the A or T nucleotide in this motif. In patients, the T and A are equally targeted (70 vs. 69 mutations, respectively) whereas in controls, A is clearly more targeted (51 T vs. 99 A mutations) (χ^2 test, $P < 0.01$, Table III). This difference was not observed in the reverse complementary motif, AT, nor the other two WA/TW motifs, AA and TT (unpublished data). When the flanking sequences of each TA motif are taken into account, the difference in targeting of the A/T nucleotides within the motif was most striking in four short DNA sequences (Table III, footnote a). In patients, the T is more targeted than A (34 vs. 18, respectively) whereas in controls, A is the preferred target (19 T vs. 38 A, Table III). Interestingly, the common feature of these four sequences is that the TA motif (bold) partially overlaps with the RGYW motif (underlined) (i.e., two are **TA**GCA and the remaining two are AGC**TA**T). This suggests that the loss of the A preference on the coding strand in ATRD patients might be a result of differences in the mechanism generating A/T mutation within these sequences.

We subsequently analyzed the frequency of mutations in each of the 64 possible trinucleotide combinations (Table S1, available at http://www.jem.org/cgi/content/full/jem.20050595/DC1). The most targeted trinucleotides, in both controls and patients, were AGC, GTA, GCT, TAG, and GGT. These are all related to the known SHM hotspot motifs (RGYW/WRYC and WA/TW) (32, 33). Significant differences were observed between the patients and controls in targeting the A nucleotides in CTA (↓ in ATRD) and TAG (↓ in ATRD) (Table S1), two trinucleotides that are included within the **TA**GCA and AGC**TA**T sequences, supporting the aforementioned observations on TA motif targeting. In addition, significant differences were found in targeting of the trinucleotide TTT (in ATRD) and the T bases in two additional trinucleotides, ATC (in ATRD) and CTC (in ATRD) (χ^2 test, $P < 0.05$ in all cases). These increases in mutations of T nucleotides may also contribute to the observed reduction of the A/T strand bias, although in this instance the triplet sequences are not associated with the previously recognized SHM hotspots.

Characteristics of the CDR3 in B cells from ATRD patients

Diversity in the CDR3 region in clones derived from the ATRD patients was also analyzed. The CDR3 contains contributions from the VH, D, and JH gene segments and nucleotides added by TDT. All clones were in-frame rearrangements. The average length of the CDR3 was 15.7 ± 2.9 aa in the ATRD clones, which is similar to those from

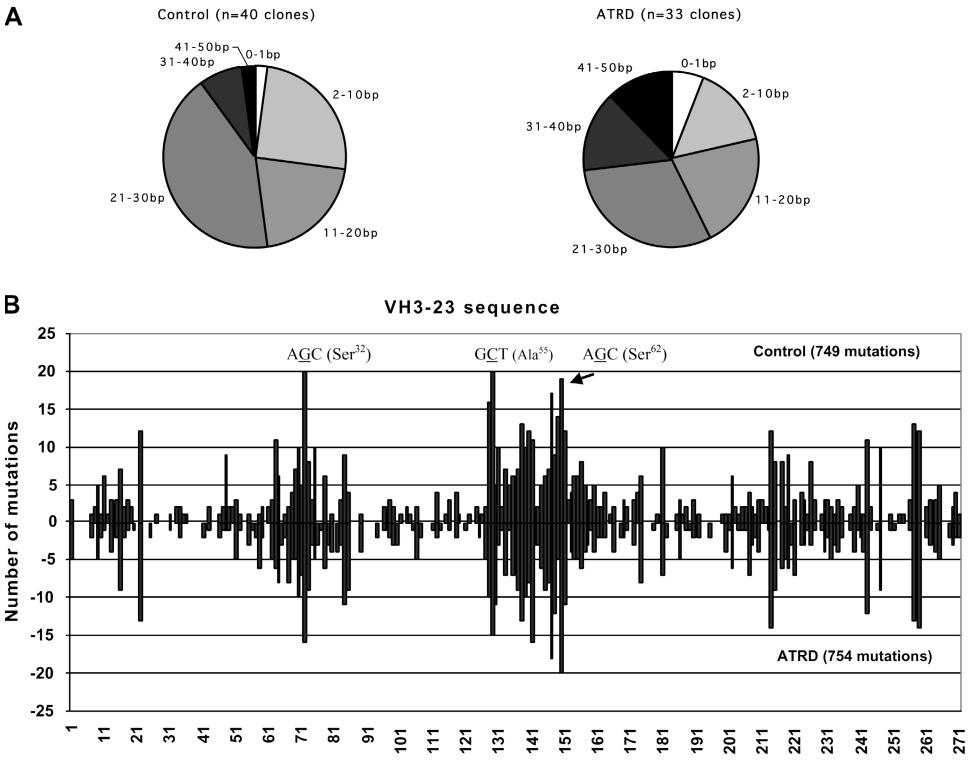

C

Controls (%)							ATRD patients (%)						
To:	T	C	A	G	Total	Corrected	To:	T	C	A	G	Total	Corrected
From:							From:						
T	/	7.7	2.0	4.4	14.2	16.8	T	/	**11.1***	**3.8***	4.5	**19.5****	**23.0****
C	12.7	/	3.3	8.9	25.0	24.9	C	12.5	/	3.2	8.2	23.9	23.7
A	5.9	5.3	/	14.0	25.2	29.9	A	5.3	5.2	/	11.3	21.8	25.6
G	3.3	10.9	21.4	/	35.6	28.5	G	5.0	11.8	18.0	/	34.9	27.7
Total	21.9	24.0	26.7	27.4	100		Total	22.8	28.1	25.1	24.0	100	
Mutations at G or C sites					61%		Mutations at G or C sites					59%	
Transitions					56%		Transitions					53%	

Figure 3. Pattern of mutations introduced in the VH3-23-Cγ transcripts. (A) Pie charts demonstrate the proportion of clones carrying the indicated number of mutations. (B) Distribution of mutations in VH3-23-Cγ transcripts in controls (above the zero line) and ATRD patients (below the zero line). Nucleotides are numbered from the third base of codon 10 of the VH3-23 coding region. The number of mutations at each position is plotted and the major hot spots are highlighed. (C) Nature of base substitutions in the VH3-23 genes. The germline sequence used for comparison contains 21.4% A, 31.7% G, 21.4% T, and 25.5% C. Correction: values presented in the column were corrected to represent a sequence with equal amounts of the four nucleotides. Statistical analysis was performed using χ^2 test. Numbers that are significantly different from controls are bold. *$P < 0.05$, **$P < 0.01$.

controls (14.9 ± 4.2 aa). The average length of the N1 regions (VH-D junctions) was significantly longer in ATRD patients as compared with controls (Student's *t* test, $P < 0.05$; Table S2, available at http://www.jem.org/cgi/content/full/jem.20050595/DC1). There was however no significant difference in the length of the N2 regions (D-JH junctions) and the frequency of P nucleotides observed between patients and controls (Table S2). Thus, the V(D)J coding joints seem to be largely normal in ATRD patients.

Functional comparison of ATR and ATM in CSR and SHM

We have previously analyzed the in vivo patterns of CSR junctions and mutations in the VH regions in A-T patients (ATM defective) using a similar experimental design, (9, 24) and these results were compared with those derived from the ATRD patients (Table IV).

The number of Sμ-Sα fragments and serum levels of immunoglobulins are highly variable in A-T patients (9). About half of the patients have no detectable serum IgA,

Table III. Number of mutations at each base of the TA motifs

	Controls				ATRD			
	Number of mutations occurring at				Number of mutations occurring at			
TA motif	T	A	Total	T/A	T	A	Total	T/A
TA-15	3	7	10	0.4	2	9	11	0.2
TA-133	7	5	12	1.4	7	1	8	7.0
TA-139	10	12	22	0.8	10	8	18	1.3
TACT-154	6	8	14	0.8	5	6	11	0.8
TACT**A**-158	2	3	5	0.7	3	1	4	3.0
TA-218	2	9	11	0.2	5	6	11	0.8
TA-258	2	12	14	0.2	4	14	18	0.3
TA-260	0	2	2	0	0	2	2	0
TA-263	0	3	3	0	0	4	4	0
Total	32	61	93	0.5	36	51	86	0.7
T**A**GCA-67[a]	2	4	6	0.5	8	5	13	1.6
AGCT**A**T-74[a]	3	10	13	0.3	3	5	8	0.6
AGCT**A**T-130[a]	5	10	15	0.5	11	3	14	**3.7**[b]
T**A**GCA-148[a]	9	14	23	0.6	12	5	17	**2.4**[b]
Total	19	38	57	0.5	34	18	52	**1.9**[c]
TA-Total	51	99	150	0.5	70	69	139	**1.0**[d]

Statistical analysis was performed using χ^2 test. T/A ratios that are significantly different from controls are bold. TA motifs analyzed are bold and the RGYW/WRCY motifs are underlined.

[a]TA motif that is partially overlaps with a RGYW motif.

[b]$P < 0.05$.

[c]$P < 0.001$.

[d]$P < 0.01$.

whereas the remainder of patients show subnormal to normal levels of IgA. However, they all show aberrant S junctions, with increased usage of microhomology and reduced number of mutations/insertions at the Sμ-Sα junctions (9). Thus, the defect in CSR in A-T patients is probably not only quantitative, but also qualitative. In ATRD patients, the number of Sμ-Sα fragments and serum levels of immunoglobulins are normal. However, ATRD2 showed low levels of antipneumococcal antibodies after immunization, which might be due to a less efficient switching to IgG2 (unpublished data). Furthermore, the Sμ-Sα junctions showed a similar trend in microhomology usage to those from A-T patients, although not as dramatic (Fig. 2 and Tables I and IV). However, the almost complete absence of 0 bp homologies (4.5% in A-T vs. 41.0% in ATRD, χ^2 test, $P < 0.001$) and the large proportion of Sμ-Sα fragments exhibiting ≥10 bp homology (30% in A-T vs. 3% in ATRD, χ^2 test, $P < 0.01$) were not found in ATRD patients. Another notable difference is that although the frequency of junctional mutations (±15 bp) was reduced in both patient groups, the proportion of junctions with insertions was reduced in patients with A-T (2 vs. 25% in controls, χ^2 test, $P < 0.01$), but not in those with ATRD (23%). Mutations close to the S junctions and 1–3 bp insertions thus seem to represent features of different repair mechanisms. These data indicate that both ATM and ATR are involved in end joining during CSR, but appear to play both similar and disparate roles in the process.

The SHM-like mutations in the Sμ regions are significantly reduced in both patient groups. The general pattern of base substitutions is altered in A-T patients, with more mutations occurring at A/T sites (56 vs. 37% in controls) and shows a strong preference for transitions (86 vs. 59%) (24). In ATRD patients, there are more mutations occurring at G/C (72%) sites, although the rate of transitions is still normal (64%). It is also worth noting that the preferred targets for SHM-like mutations within RGYW/WRCY motifs (commonly AGCT motifs in these data) are also different between the two patient groups. Almost all the mutations in ATRD patients target the second and third nucleotides (93%), whereas close to half of the mutations from A-T patients target the last T in these motifs (42%). In controls, 83% of the mutations occur at the second and third nucleotides and 5% at the last T in the RGYW/WRCY motifs. Therefore, ATR, like ATM, seems to be involved in the generation of mutations in the Sμ region, although probably via a different mechanism.

A-T patients show a normal frequency and a largely normal pattern of SHM in the VH regions (24), whereas in ATRD patients, the mutation pattern was clearly altered. As for the targeting of individual trinucleotides, A-T patients showed a similar pattern as controls (unpublished data), whereas in

Table IV. Roles of ATM and ATR in CSR, SHM, and V(D)J recombination

	A-T patients	ATRD patients
CSR		
Serum IgA and IgG level	Not detectable to normal	Normal
No. of clones switched to IgA	↓[a] to Normal	Normal
Sμ-Sα junctions		
Average microhomology	↑[b] 7.2 ± 6.0 bp	↑[a] 3.0 ± 3.8 bp
Shift of Sμ breakpoints	Yes[b]	Yes[c]
Junctional mutations	↓[c]	↓[a]
Junctional insertions	↓[c]	Normal
Sμ-Sγ junctions		
Average microhomology	↑[b] 2.5 ± 1.7 bp	↑[a] 1.8 ± 2.0 bp
Junctional mutations	↓[a]	(↓)
Junctional insertions	(↓)	Normal
SHM-like mutation in Sμ region		
Frequency	↓[b]	↓[b]
Pattern	Altered, A/T biased, transition biased	G/C biased (↓) A mutations
SHM		
Frequency	Normal	(↑)
Pattern	Largely normal	Altered, lost A/T strand bias
V(D)J recombination		
Coding joints	Normal	Largely normal, ↑[a] length of N1 region

Statistical analysis was performed using χ^2 test or Student's *t* test (for average length of microhomology). The numbers that are significantly different from controls are marked by or ↓. (↑) or (↓), increased or decreased as compared to the controls, but not to a statistically significant degree.
[a]$P < 0.05$.
[b]$P < 0.001$.
[c]$P < 0.01$.

ATRD patients the targeting of A or T bases in certain trinucleotides was significantly altered.

DISCUSSION

In this study, we have, for the first time, shown a role for ATR in CSR and SHM. The study also revealed interesting functional differences between ATM and ATR-mediated signaling; the ATM-dependent pathway is mainly used in the end joining process in CSR, whereas the ATR-dependent pathway appears to be involved in both CSR and SHM.

The functional roles of ATM and ATR have been extensively studied in the general DNA damage response. Both are structurally and functionally related with overlapping substrates and have therefore been suggested to operate within the same pathway (21, 34, 35). However, while ATM exclusively responds to DSBs induced by ionizing radiation and some radiomimetic agents, ATR is also activated by single-stranded DNA (ssDNA) generated during DNA replication or by agents such as UV irradiation that produce bulky lesions (35, 36). There also seem to be kinetic differences between the two kinases when responding to different forms of DNA damage. Both ATM and ATR phosphorylate p53 on serine-15 in response to ionizing radiation, but ATM initiates the process whereas ATR dominates the phosphorylation process at later stages (36). However, in response to a methylating agent, temozolomide, ATM is activated later than ATR (37). Furthermore, the function of ATR is dependent on an accessory protein, ATRIP (ATR-interacting protein), which is phosphorylated by ATR (38).

The different pattern of CSR junctions and SHM in the VH regions, when ATM or ATR is defective, could potentially be explained by the known differences between the two kinases. In CSR, a DSB intermediate appears to be part of the reaction (39), and ATM may thus play a major role in the initial stage of the repair process. However, by responding to the ssDNA resulting from processed DSBs, ATR will reinforce the ATM response, resulting in a potentiation of the reaction. In SHM, DSBs seem not to be prominent intermediates, instead, SSBs or single strand nicks appear to be essential (40–42). ATM, which only responds to DSBs, is thus dispensable for the SHM process. Alternately, ATR, when complexed with ATRIP, is recruited to ssDNA by RPA (43), a factor that targets AID to SHM motifs (44). When ATR activity is absent, or impaired (as in our patients, who carry hypomorphic mutations), the SHM pattern is perturbed.

The different patterns of Sμ-Sα junctions in A-T and ATRD patients may help to further dissect the four end joining pathways we have previously proposed (9, 45). The first pathway entails a "blunt end" direct joining mechanism, where no sequence homology is needed and the two DNA ends are either joined precisely or where 1–3 bp (mostly 1 bp) insertions are introduced. The second pathway involves joining of partially complementary "staggered" DNA ends by a mechanism involving alignment of residual complementarities (1–3 bp) in 3′ or 5′ overhangs, filling in of any remaining gaps and ligation. This process is imprecise, and mutations are frequently introduced at, or close to, the switch junctions. The third pathway has precise joining of complementary DNA ends with a short sequence homology (1–3 bp), probably through simple religation, with no mutations or insertions being introduced at, or close to, the junctions. The fourth pathway is an alternative joining of noncomplementary ends, by resecting the DNA ends until homology suitable for end joining is revealed where at least 4 bp of microhomology is observed at the S junction. In B cells from healthy individuals, the first pathway is dominant (44% of Sμ-Sα events) and the other three are used with similar frequencies (~20%). The first pathway, "blunt end" direct joining is markedly impaired in A-T patients, but normal in ATRD patients, suggesting that this process is strictly dependent on a rapid, efficient response by ATM. The second

("staggered end" joining involving misalignment and filling in) pathway is less often used in both A-T and ATRD patients (9 and 3%, respectively, as compared with 16% in controls), suggesting that both ATM and ATR are required for processing of partially complementary ends. The third pathway, involving simple religation, is not affected. However, usage of the fourth pathway, involving ≥4 bp microhomology, is increased in both patient groups (61 and 38%, respectively, as compared with 20% in controls). Interestingly, in contrast with A-T patients, the CSR junctions from ATRD patients only show an increased usage of microhomology up to 9 bp, suggesting that there may be yet another pathway or subpathway, requiring longer microhomologies (≥10 bp), that may be dependent on ATR.

Although the aforementioned end joining pathways in CSR are still speculative, it could provide a platform when comparing data from patients with genetic defects that affect specific DNA damage response pathways. In patients lacking DNA ligase IV, a critical component of the NHEJ machinery, the pattern of Sμ-Sα junctions is similar to that of A-T patients (45). The first and second pathways are almost not used at all, the third pathway is not affected (20%), and the fourth pathway is dominant (73%), suggesting that the "blunt end" and "staggered end" joining with short, noncomplementary ends are strictly dependent on the classical NHEJ machinery. The third pathway, which is not affected by ATM, ATR, or DNA ligase IV, is impaired in NBS (Nbs1 defective, 4%) and, to a lesser degree, in ATLD patients (Mre11 defective, 11%) (13), suggesting that simple religation involving short homologous ends in CSR is probably, as described in the yeast system (46), dependent on the Mre11–Rad50–Nbs1 complex.

However, the balance between these putative different pathways is dependent not only on the factors available but also on the degree of homology between the S regions. The microhomology based end joining is much more prominent at Sμ-Sα as compared with Sμ-Sγ junctions in all patient groups, probably because of the higher degree of homology between Sμ and Sα as compared with Sμ and Sγ regions (45). The likelihood of obtaining a 7-, 10-, or 15-bp microhomology between the Sμ-Sα regions is 8, 270, and >1,000-fold higher than in the Sμ-Sγ regions. Furthermore, the mutation pattern at, or close to, the Sμ-Sγ junctions is also different from the Sμ-Sα junctions in normal controls (45, 47). Moreover, in A-T and ATRD patients, the Sμ-Sγ junctions tend to use more microhomologies, whereas in Lig4D patients, the Sμ-Sγ junctions mainly show an increased frequency of 1-bp insertions (45). Thus, the Sμ-Sα and Sμ-Sγ junctions are resolved differently in controls and patients with various defects in their DNA repair systems. In mice, the Sα regions also show a much higher degree of homology with Sμ, than does Sγ, and the microhomology-based pathway would be a more attractive alternative for Sμ/Sα recombination when the normal repair pathways is impaired. However, in the various mouse knockout models described to date, Sμ-Sα junctions have not been analyzed in as much as detail as Sμ-Sγ1 and Sμ-Sγ3 junctions (10, 11, 16–18, 48). An analysis of Sμ-Sα junctions from mouse B cells deficient for H2AX and 53BP1, where no equivalent human disease model is available, would thus facilitate our understanding of the regulation of ATM–ATR-dependent pathways in CSR.

The loss of strand polarity in targeting A/T pairs in the VH regions from ATRD patients is an interesting finding. The mechanism underlying the strand polarity at A/T pairs (i.e., with mutations at A on the coding strand being nearly twice as frequent as mutations at T [32]) is not well understood. One possibility is that the A/T bias is a consequence of an initial preferential targeting of dCs by AID in the nontranscribed strand (49). Alternatively, it may reflect the strand preference of transcription-linked repair, where an abasic site created by excising a U residue from the transcribed DNA strand of U-A pairs is treated differently (repaired or mutated) from an abasic site located on the nontranscribed strand (42). Because ATR and AID can both associate with RPA, this raises several possible explanations; ATR could be acting as early as at the initial AID targeting stage by phosphorylating RPA (50) or by regulating its intranuclear translocation (51). Alternately, RPA recruits ATR–ATRIP complex to sites of DNA damage (43) so ATR involvement could be postinitiation. Two other PIKKs kinases, ATM and DNA-PKcs, have also been implicated in the DNA damage-induced phosphorylation of RPA (for review see reference 52). However, as the SHM patterns are largely normal in cells deficient in ATM or DNA-PKcs (24, 25), their kinase activities are probably not required in this process. An alternative role for ATR could be at a later stage, by interacting with or recruiting members of the mismatch repair pathway, such as MSH2 (53, 54) and MSH6 or polymerase (pol) η, all of which have been implicated in generating mutations at A/T sites (42, 55–57). Pol η in particular is thought to contribute to strand bias of A versus T nucleotides by generating more mutations from A than T on the nontranscribed strand (58). However, cells deficient in various mismatch repair proteins and pol η show reduced rates of mutation at both A and T nucleotides (42, 56), whereas in ATRD cells, the mutation load on A and T nucleotides is normal but an increased ratio of T/A targeting is observed. Loss of strand bias has also previously been noted in a mutating B cell line, Ramos (59). Interestingly, the *ATR* gene is not expressed in this cell line, whereas *MSH2*, *MSH6* (unpublished data) and *pol η* (60) transcripts are readily detected. However, the pattern of mutations observed in Ramos cells is strongly biased to G/C (82%), similar to those in MSH2, MSH6, or pol η–deficient cells, suggesting that in addition to ATR, deficiency of other DNA repair factors may account for the mutation pattern observed in this cells line. Together, ATR is unlikely to be an "A/T mutator," but rather, recruits "A/T mutators," such as pol η, preferentially to the transcribed strand at specific sequences. Because ATR may be linked to AID via RPA, it is logical that its effects are more noticeable near the AID target motifs (WRC/GYW) (61, 62), hence the finding in this report that

loss of ATR reduces A/T strand bias at the **TA**GCA or AGC**TA**T sequences.

Another possibility that needs to be excluded is that the altered mutation pattern in ATRD cells is the result of a bias introduced by studying only the expressed VH genes. To address this question, an analysis of the noncoding regions of the heavy chain locus such as the JH4 intron sequence (57) was attempted. We were able to obtain a small number of purified $CD27^+$ B cells from two patients, ATRD1 and ATRD2, and amplified the JH4 intron sequence downstream of the rearranged VH3-23 gene as described previously (57). In controls ($n = 5$), an average frequency of 16/1,000 bp of mutations was observed, which is similar to that published previously (57). However, very few mutations were identified in the patients even after screening a large number of clones ($n = 66$), precluding the possibility to compare the mutation pattern. Nevertheless, although WA motifs are common in the 320 bp of the JH4 intron sequence, there are only three TA motifs and none of these is associated with the RGYW motif. Thus, one would not expect to reproduce the specific pattern observed in the VH regions in ATRD patients.

The Sμ region is another noncoding region that has been used to analyze nonselected, SHM-like mutations (56, 57). In the limited number of mutations we observed in the Sμ region, away from the breakpoints, we did observe a reduced number of mutations at A nucleotides (T/A ratio 1:1). However, the SHM-like mutations observed in the Sμ region are probably introduced at an early stage during CSR, in a process that may share some of the factors with SHM but which is still mechanistically different (24). Thus, an altered mutation pattern in the Sμ region may not necessarily be the result of changes in the SHM machinery.

The Seckel syndrome is a clinically and genetically heterogeneous disorder where at least four susceptibility loci have been suggested (63–66). To date however, mutation in *ATR* is the only genetic defect identified. Of the 70 patients described worldwide, only 5 patients carry mutations in the *ATR* gene. However, a recent study has shown that there are remarkably overlapping phenotypes between a panel of Seckel syndrome cell lines (with no defect in *ATR*) and an ATRD-Seckel cell line (67), suggesting that the disease is indeed caused by defects in the ATR-signaling pathway. It would therefore be of considerable interest to study the CSR and SHM patterns in additional patients with the Seckel syndrome, where the gene mutated may be one of the other factors involved in the ATR-dependent pathway, including *ATRIP*, *RPA*, *RAD17*, *chk1*, *53BP1,* and *H2AX*.

In conclusion, V(D)J recombination, SHM and CSR may share some of the molecular mechanisms involved but are differentially regulated. ATR is probably dispensable for V(D)J recombination, but may play some role in the end joining machinery in CSR and in SHM.

MATERIALS AND METHODS

Patient material. The study included three patients from one family with Seckel syndrome with mutations in the *ATR* gene. The clinical details of the patients (ATRD1, ATRD2, and ATRD3 referred to as V3, V6 and V4 in reference 66) have been described previously (26, 66). The mutation in the *ATR* gene in these patients is a homozygous replacement within exon 9 (2101 A>G) that alters *ATR* splicing, resulting in markedly reduced levels of normal transcripts and protein (26). The serum levels of immunoglobulin classes are normal in the studied patients (66). Lymphocyte count was available from one patient, ATRD2, and the number of B cells was slightly above the upper normal range, whereas the number of T cells was at the lower normal range. The genetic characterization and immunoglobulin levels in the A-T patients discussed in this study have all been described previously (8, 9). The institution review board at the Karolinska Institute approved the study.

Amplification of Sμ-Sα and Sμ-Sγ fragments. Genomic DNA was purified from peripheral blood cells from the ATRD patients. The amplification of Sμ-Sα fragments from in vivo switched cells was performed as described previously (9, 30). In brief, two pairs of Sμ- and Sα-specific primers were used in a nested PCR assay. The number of Sμ-Sα fragments was determined from 10 reactions run in parallel using DNA (30 ng per reaction) from each individual and represents a random amplification of in vivo switched clones. The number of IgA positive cells in 30 ng of genomic DNA prepared from normal peripheral blood cells was estimated to be 30–60 (assuming that 40% peripheral blood cells are lymphocytes, 10–20% of the lymphocytes are B cells and 5% of the B cells are IgA^+). One or two Sμ-Sα fragments were normally amplified in one lane, when 30 ng of DNA was added in one reaction. This sensitivity, 15–30 copies, is in the same order of sensitivity as we have previously estimated using a human IgA1–producing cell line (30). The same cell line was also used to assess the fidelity of the nested PCR reaction and the PCR error rate was 0.9/1,000 nucleotides (30).

The Sμ-Sγ fragments were amplified as described previously (68) with addition of Sγ1-specific and Sγ2-specific primers (45).

Analysis of the Sμ-Sα and Sμ-Sγ junctions. The PCR-amplified S fragments were gel purified, cloned, and sequenced as described previously (9). The breakpoints were determined by aligning the switch fragment sequences with the Sμ (X54713)/Sα1 (L19121)/Sα2 (AF030305) or Sμ/Sγ1 (U39737)/Sγ2 (U39934)/Sγ3 (U39935)/Sγ4 (Y12547-52) sequences. Analysis of microhomology usage at the junctions and mutations ±15 bp around the junction and upstream Sμ region were performed as described previously (9, 24).

RNA isolation and PCR amplification of VH3-Cγ transcripts. Total RNA was extracted from PBL using RNeasy RNA purification kits (QIAGEN) and first-strand cDNA synthesis was performed with a CγA primer (5′-GTCCTTGACCAGGCAGCCCAG-3′) using a cDNA synthesis kit (GE Healthcare). The primers used for amplification of VH3-Cγ and VH3-23-Cγ transcripts were VH3-consensus (5′-aatctagaGGTGCAGCTGGTGGAG-TC-3′) or VH3-23 (5′-tctagaGGCTGAGCTGGCTTTTTCTTGTGG-3′) and CγB (5′-cagtcgacAAGACCGATGGGCCCTTGGTGG-3′). The oligonucleotides contained a restriction site, (underlined, a XbaI site in the VH3-consensus or VH3-23 primer and a SalI site in the CγB primer) for directional cloning of the PCR products. Amplification was performed in 35 cycles, each cycle consisting of 94°C for 50 s, 62°C for 1 min, and 72°C for 1 min. A high fidelity Vent DNA polymerase (New England BioLabs) was used in all PCR amplifications of the VH region transcripts.

Analysis of the VH-Cγ clones. The PCR products were purified and cloned into the Bluescript II KS (+) vector (Stratagene) and transformed into JM 109 competent cells. The resulting clones were screened by PCR amplification (VH3-consensus/VH3-23 and CγB) and positive clones were sequenced by an automated fluorescent sequencer in the MWG Co. using a Bigdye terminator cycle sequencing kit (Perkin Elmer). Sequence analysis was performed using the IMGT/V-QUEST (http://imgt.cines.fr) (69) to align the VH-CγB sequences to their closest germline VH, D, and JH segment counterparts. The immunoglobulin V(D)J junctional sequences were analyzed by the IMGT/JunctionAnalysis tool, available at http://imgt.cines.fr.

When analyzing the trinucleotides targeting, mutated VH3-23 sequences were aligned beneath the germline VH3-23 region gene and a raw test file of the alignment created. This file was imported into a Microsoft Excel spreadsheet and computations of the number of each type of nucleotide substitution and the composition of the flanking sequences around these substitutions were performed using macros in Excel (Visual Basic). Computations of percentage differences and χ^2 analysis were also performed using Excel.

Online supplemental material. Table S1 shows the number of mutations at each base of all trinucleotides. Table S2 shows the characteristics of the CDR3 regions in cells from ATRD patients and controls. Fig. S1 shows the sμ-sα junctions from ATRD patients. Online supplemental material is available at http://www.jem.org/cgi/content/full/jem.20050595/DC1.

We thank Prof. J. Stavnezer for helpful comments on the manuscript and Dr. R. Mehr for suggestions on data analysis.

This work was supported by the Swedish Research Council, the Swedish Society for Medical Research (SSMF), and the Swedish Doctors Association.

The authors have no conflicting financial interests.

Submitted: 22 March 2005
Accepted: 23 November 2005

REFERENCES

1. Lieber, M.R., Y. Ma, U. Pannicke, and K. Schwarz. 2003. Mechanism and regulation of human non-homologous DNA end-joining. *Nat. Rev. Mol. Cell Biol.* 4:712–720.
2. Muramatsu, M., K. Kinoshita, S. Fagarasan, S. Yamada, Y. Shinkai, and T. Honjo. 2000. Class switch recombination and hypermutation require activation-induced cytidine deaminase (AID), a potential RNA editing enzyme. *Cell.* 102:553–563.
3. Di Noia, J., and M.S. Neuberger. 2002. Altering the pathway of immunoglobulin hypermutation by inhibiting uracil-DNA glycosylase. *Nature.* 419:43–48.
4. Rada, C., G.T. Williams, H. Nilsen, D.E. Barnes, T. Lindahl, and M.S. Neuberger. 2002. Immunoglobulin isotype switching is inhibited and somatic hypermutation perturbed in UNG-deficient mice. *Curr. Biol.* 12:1748–1755.
5. Petersen-Mahrt, S.K., R.S. Harris, and M.S. Neuberger. 2002. AID mutates *E. coli* suggesting a DNA deamination mechanism for antibody diversification. *Nature.* 418:99–103.
6. Chaudhuri, J., and F.W. Alt. 2004. Class-switch recombination: interplay of transcription, DNA deamination and DNA repair. *Nat. Rev. Immunol.* 4:541–552.
7. Savitsky, K., A. Bar-Shira, S. Gilad, G. Rotman, Y. Ziv, L. Vanagaite, D.A. Tagle, S. Smith, T. Uziel, S. Sfez, et al. 1995. A single ataxia telangiectasia gene with a product similar to PI-3 kinase. *Science.* 268: 1749–1753.
8. Lähdesmäki, A., K. Arinbjarnarson, J. Arvidsson, M.E. Segaier, A. Fasth, E. Fernell, D. Gustafsson, V.-A. Oxelius, K. Risberg, J. Yuen, et al. 2000. Ataxia-telangiectasia surveyed in Sweden. [In Swedish.] Lakartidningen. 97:4461–4467.
9. Pan, Q., C. Petit-Frere, A. Lähdesmäki, H. Gregorek, K.H. Chrzanowska, and L. Hammarström. 2002. Alternative end joining during switch recombination in patients with ataxia-telangiectasia. *Eur. J. Immunol.* 32:1300–1308.
10. Reina-San-Martin, B., H.T. Chen, A. Nussenzweig, and M.C. Nussenzweig. 2004. ATM is required for efficient recombination between immunoglobulin switch regions. *J. Exp. Med.* 200:1103–1110.
11. Lumsden, J.M., T. McCarty, L.K. Petiniot, R. Shen, C. Barlow, T.A. Wynn, H.C. Morse III, P.J. Gearhart, A. Wynshaw-Boris, E.E. Max, and R.J. Hodes. 2004. Immunoglobulin class switch recombination is impaired in Atm-deficient mice. *J. Exp. Med.* 200:1111–1121.
12. Petersen, S., R. Casellas, B. Reina-San-Martin, H.T. Chen, M.J. Difilippantonio, P.C. Wilson, L. Hanitsch, A. Celeste, M. Muramatsu, D.R. Pilch, et al. 2001. AID is required to initiate Nbs1/γ-H2AX focus formation and mutations at sites of class switching. *Nature.* 414:660–665.
13. Lähdesmäki, A., A.M. Taylor, K.H. Chrzanowska, and Q. Pan-Hammarström. 2004. Delineation of the role of the Mre11 complex in class switch recombination. *J. Biol. Chem.* 279:16479–16487.
14. Reina-San-Martin, B., M.C. Nussenzweig, A. Nussenzweig, and S. Difilippantonio. 2005. Genomic instability, endoreduplication, and diminished Ig class-switch recombination in B cells lacking Nbs 1. *Proc. Natl. Acad. Sci. USA.* 102:1590–1595.
15. Kracker, S., Y. Bergmann, I. Demuth, P.O. Frappart, G. Hildebrand, R. Christine, Z.Q. Wang, K. Sperling, M. Digweed, and A. Radbruch. 2005. Nibrin functions in Ig class-switch recombination. *Proc. Natl. Acad. Sci. USA.* 102:1584–1589.
16. Reina-San-Martin, B., S. Difilippantonio, L. Hanitsch, R.F. Masilamani, A. Nussenzweig, and M.C. Nussenzweig. 2003. H2AX is required for recombination between immunoglobulin switch regions but not for intra-switch region recombination or somatic hypermutation. *J. Exp. Med.* 197:1767–1778.
17. Manis, J.P., J.C. Morales, Z. Xia, J.L. Kutok, F.W. Alt, and P.B. Carpenter. 2004. 53BP1 links DNA damage-response pathways to immunoglobulin heavy chain class-switch recombination. *Nat. Immunol.* 5:481–487.
18. Ward, I.M., B. Reina-San-Martin, A. Olaru, K. Minn, K. Tamada, J.S. Lau, M. Cascalho, L. Chen, A. Nussenzweig, F. Livak, et al. 2004. 53BP1 is required for class switch recombination. *J. Cell Biol.* 165: 459–464.
19. Rolink, A., F. Melchers, and J. Andersson. 1996. The SCID but not the RAG-2 gene product is required for Sμ-Sε heavy chain class switching. *Immunity.* 5:319–330.
20. Manis, J.P., D. Dudley, L. Kaylor, and F.W. Alt. 2002. IgH class switch recombination to IgG1 in DNA-PKcs-deficient B cells. *Immunity.* 16: 607–617.
21. Abraham, R.T. 2001. Cell cycle checkpoint signaling through the ATM and ATR kinases. *Genes Dev.* 15:2177–2196.
22. de Klein, A., M. Muijtjens, R. van Os, Y. Verhoeven, B. Smit, A.M. Carr, A.R. Lehmann, and J.H. Hoeijmakers. 2000. Targeted disruption of the cell-cycle checkpoint gene ATR leads to early embryonic lethality in mice. *Curr. Biol.* 10:479–482.
23. Brown, E.J., and D. Baltimore. 2000. ATR disruption leads to chromosomal fragmentation and early embryonic lethality. *Genes Dev.* 14: 397–402.
24. Pan-Hammarström, Q., S. Dai, Y. Zhao, I.F. van Dijk-Härd, R.A. Gatti, A.L. Børresen-Dale, and L. Hammarström. 2003. ATM is not required in somatic hypermutation of VH, but is involved in the introduction of mutations in the switch μ region. *J. Immunol.* 170:3707–3716.
25. Bemark, M., J.E. Sale, H.J. Kim, C. Berek, R.A. Cosgrove, and M.S. Neuberger. 2000. Somatic hypermutation in the absence of DNA-dependent protein kinase catalytic subunit (DNA-PK(cs)) or recombination-activating gene (RAG)1 activity. *J. Exp. Med.* 192:1509–1514.
26. O'Driscoll, M., V.L. Ruiz-Perez, C.G. Woods, P.A. Jeggo, and J.A. Goodship. 2003. A splicing mutation affecting expression of ataxia-telangiectasia and Rad3-related protein (ATR) results in Seckel syndrome. *Nat. Genet.* 33:497–501.
27. Bobabilla-Morales, L., A. Corona-Rivera, J.R. Corona-Rivera, C. Buenrostro, T.A. Garcia-Cobian, E. Corona-Rivera, J.M. Cantu-Garza, and D. Garcia-Cruz. 2003. Chromosome instability induced in vitro with mitomycin C in five Seckel syndrome patients. *Am. J. Med. Genet. A.* 123:148–152.
28. Casper, A.M., S.G. Durkin, M.F. Arlt, and T.W. Glover. 2004. Chromosomal instability at common fragile sites in Seckel syndrome. *Am. J. Hum. Genet.* 75:654–660.
29. Hayani, A., C.R. Suarez, Z. Molnar, M. LeBeau, and J. Godwin. 1994. Acute myeloid leukaemia in a patient with Seckel syndrome. *J. Med. Genet.* 31:148–149.
30. Pan, Q., C. Petit-Frere, S. Dai, P. Huang, H.C. Morton, P. Brandtzaeg, and L. Hammarström. 2001. Regulation of switching and production of IgA in human B cells in donors with duplicated α1 genes. *Eur. J. Immunol.* 31:3622–3630.
31. Betz, A.G., M.S. Neuberger, and C. Milstein. 1993. Discriminating intrinsic and antigen-selected mutational hotspots in immunoglobulin V genes. *Immunol. Today.* 14:405–411.

32. Milstein, C., M.S. Neuberger, and R. Staden. 1998. Both DNA strands of antibody genes are hypermutation targets. *Proc. Natl. Acad. Sci. USA*. 95:8791–8794.
33. Rogozin, I.B., Y.I. Pavlov, K. Bebenek, T. Matsuda, and T.A. Kunkel. 2001. Somatic mutation hotspots correlate with DNA polymerase η error spectrum. *Nat. Immunol*. 2:530–536.
34. Shiloh, Y. 2003. ATM and related protein kinases: safeguarding genome integrity. *Nat. Rev. Cancer*. 3:155–168.
35. Shiloh, Y. 2001. ATM and ATR: networking cellular responses to DNA damage. *Curr. Opin. Genet. Dev*. 11:71–77.
36. Tibbetts, R.S., K.M. Brumbaugh, J.M. Williams, J.N. Sarkaria, W.A. Cliby, S.Y. Shieh, Y. Taya, C. Prives, and R.T. Abraham. 1999. A role for ATR in the DNA damage-induced phosphorylation of p53. *Genes Dev*. 13:152–157.
37. Caporali, S., S. Falcinelli, G. Starace, M.T. Russo, E. Bonmassar, J. Jiricny, and S. D'Atri. 2004. DNA damage induced by temozolomide signals to both ATM and ATR: role of the mismatch repair system. *Mol. Pharmacol*. 66:478–491.
38. Cortez, D., S. Guntuku, J. Qin, and S.J. Elledge. 2001. ATR and ATRIP: partners in checkpoint signaling. *Science*. 294:1713–1716.
39. Wuerffel, R.A., J. Du, R.J. Thompson, and A.L. Kenter. 1997. Ig Sγ3 DNA-specifc double strand breaks are induced in mitogen-activated B cells and are implicated in switch recombination. *J. Immunol*. 159:4139–4144.
40. Faili, A., S. Aoufouchi, Q. Gueranger, C. Zober, A. Leon, B. Bertocci, J.C. Weill, and C.A. Reynaud. 2002. AID-dependent somatic hypermutation occurs as a DNA single-strand event in the BL2 cell line. *Nat. Immunol*. 3:815–821.
41. Li, Z., C.J. Woo, M.D. Iglesias-Ussel, D. Ronai, and M.D. Scharff. 2004. The generation of antibody diversity through somatic hypermutation and class switch recombination. *Genes Dev*. 18:1–11.
42. Neuberger, M.S., J.M. Di Noia, R.C. Beale, G.T. Williams, Z. Yang, and C. Rada. 2005. Somatic hypermutation at A.T pairs: polymerase error versus dUTP incorporation. *Nat. Rev. Immunol*. 5:171–178.
43. Zou, L., and S.J. Elledge. 2003. Sensing DNA damage through ATRIP recognition of RPA-ssDNA complexes. *Science*. 300:1542–1548.
44. Chaudhuri, J., C. Khuong, and F.W. Alt. 2004. Replication protein A interacts with AID to promote deamination of somatic hypermutation targets. *Nature*. 430:992–998.
45. Pan-Hammarström, Q., A.M. Jones, A. Lähdesmäki, W. Zhou, R.A. Gatti, L. Hammarström, A.R. Gennery, and M.R. Ehrenstein. 2005. Impact of DNA ligase IV on nonhomologous end joining pathways during class switch recombination in human cells. *J. Exp. Med*. 201:189–194.
46. Haber, J.E. 1999. Sir-Ku-itous routes to make ends meet. *Cell*. 97: 829–832.
47. Pan, Q., and L. Hammarström. 1999. Targeting of human switch recombination breakpoints: implications for the mechanism of μ-γ isotype switching. *Eur. J. Immunol*. 29:2779–2787.
48. Schrader, C.E., J. Vardo, and J. Stavnezer. 2002. Role for mismatch repair proteins Msh2, Mlh1, and Pms2 in immunoglobulin class switching shown by sequence analysis of recombination junctions. *J. Exp. Med*. 195:367–373.
49. Barreto, V.M., A.R. Ramiro, and M.C. Nussenzweig. 2005. Activation-induced deaminase: controversies and open questions. *Trends Immunol*. 26:90–96.
50. Bartrand, A.J., D. Iyasu, and G.S. Brush. 2004. DNA stimulates Mec1-mediated phosphorylation of replication protein A. *J. Biol. Chem*. 279: 26762–26767.
51. Barr, S.M., C.G. Leung, E.E. Chang, and K.A. Cimprich. 2003. ATR kinase activity regulates the intranuclear translocation of ATR and RPA following ionizing radiation. *Curr. Biol*. 13:1047–1051.
52. Binz, S.K., A.M. Sheehan, and M.S. Wold. 2004. Replication protein A phosphorylation and the cellular response to DNA damage. *DNA Repair (Amst.)*. 3:1015–1024.
53. Fang, Y., C.C. Tsao, B.K. Goodman, R. Furumai, C.A. Tirado, R.T. Abraham, and X.F. Wang. 2004. ATR functions as a gene dosage-dependent tumor suppressor on a mismatch repair-deficient background. *EMBO J*. 23:3164–3174.
54. Wang, Y., and J. Qin. 2003. MSH2 and ATR form a signaling module and regulate two branches of the damage response to DNA methylation. *Proc. Natl. Acad. Sci. USA*. 100:15387–15392.
55. Zeng, X., D.B. Winter, C. Kasmer, K.H. Kraemer, A.R. Lehmann, and P.J. Gearhart. 2001. DNA polymerase η is an A-T mutator in somatic hypermutation of immunoglobulin variable genes. *Nat. Immunol*. 2: 537–541.
56. Martomo, S.A., W.W. Yang, and P.J. Gearhart. 2004. A role for msh6 but not msh3 in somatic hypermutation and class switch recombination. *J. Exp. Med*. 200:61–68.
57. Faili, A., S. Aoufouchi, S. Weller, F. Vuillier, A. Stary, A. Sarasin, C.A. Reynaud, and J.C. Weill. 2004. DNA polymerase eta is involved in hypermutation occurring during immunoglobulin class switch recombination. *J. Exp. Med*. 199:265–270.
58. Mayorov, V.I., I.B. Rogozin, L.R. Adkison, and P.J. Gearhart. 2005. DNA polymerase η contributes to strand bias of mutations of A versus T in immunoglobulin genes. *J. Immunol*. 174:7781–7786.
59. Sale, J.E., and M.S. Neuberger. 1998. TdT-accessible breaks are scattered over the immunoglobulin V domain in a constitutively hypermutating B cell line. *Immunity*. 9:859–869.
60. Zhang, W., P.D. Bardwell, C.J. Woo, V. Poltoratsky, M.D. Scharff, and A. Martin. 2001. Clonal instability of V region hypermutation in the Ramos Burkitt's lymphoma cell line. *Int. Immunol*. 13: 1175–1184.
61. Yu, K., F.T. Huang, and M.R. Lieber. 2004. DNA substrate length and surrounding sequence affect the activation-induced deaminase activity at cytidine. *J. Biol. Chem*. 279:6496–6500.
62. Pham, P., R. Bransteitter, J. Petruska, and M.F. Goodman. 2003. Processive AID-catalysed cytosine deamination on single-stranded DNA simulates somatic hypermutation. *Nature*. 424:103–107.
63. Borglum, A.D., T. Balslev, A. Haagerup, N. Birkebaek, H. Binderup, T.A. Kruse, and J.M. Hertz. 2001. A new locus for Seckel syndrome on chromosome 18p11.31-q11. 2. *Eur. J. Hum. Genet*. 9:753–757.
64. Faivre, L., M. Le Merrer, S. Lyonnet, H. Plauchu, N. Dagoneau, A.B. Campos-Xavier, J. Attia-Sobol, A. Verloes, A. Munnich, and V. Cormier-Daire. 2002. Clinical and genetic heterogeneity of Seckel syndrome. *Am. J. Med. Genet*. 112:379–383.
65. Kilinc, M.O., V.N. Ninis, S.A. Ugur, B. Tuysuz, M. Seven, S. Balci, J. Goodship, and A. Tolun. 2003. Is the novel SCKL3 at 14q23 the predominant Seckel locus? *Eur. J. Hum. Genet*. 11:851–857.
66. Goodship, J., H. Gill, J. Carter, A. Jackson, M. Splitt, and M. Wright. 2000. Autozygosity mapping of a Seckel syndrome locus to chromosome 3q22. 1-q24. *Am. J. Hum. Genet*. 67:498–503.
67. Alderton, G.K., H. Joenje, R. Varon, A.D. Borglum, P.A. Jeggo, and M. O'Driscoll. 2004. Seckel syndrome exhibits cellular features demonstrating defects in the ATR-signalling pathway. *Hum. Mol. Genet*. 13:3127–3138.
68. Pan, Q., H. Rabbani, F.C. Mills, E. Severinson, and L. Hammarström. 1997. Allotype-associated variation in the human γ3 switch region as a basis for differences in IgG3 production. *J. Immunol*. 158:5849–5859.
69. Lefranc, M.P. 2001. IMGT, the international ImMunoGeneTics database. *Nucleic Acids Res*. 29:207–209.